SUI 61-20

Department of Physics and Astronomy
STATE UNIVERSITY OF IOWA
Iowa City

COORDINATES FOR MAPPING THE DISTRIBUTION OF MAGNETICALLY TRAPPED PARTICLES*

by

Carl E. McIlwain

Department of Physics and Astronomy
State University of Iowa
Iowa City, Iowa

August 1961

* Supported in part by the Office of Naval Research (contract number N9onr 93803) and by the National Aeronautics and Space Administration (contract number NASw-17).

ABSTRACT

Dipole representations of the earth's magnetic field have been found to have insufficient accuracy for the study of magnetically trapped particles. A coordinate system consisting of the magnitude of the magnetic field B, and the integral invariant I has been found to adequately organize measurements made at different geographic locations. It is shown in the present paper, that a parameter $L = f(B,I)$ can be defined which retains most of the desirable properties of I and which has the additional property of organizing measurements along lines of force. Since the parameter L is the analog of a physical distance in a dipole field (the equatorial radius of a magnetic shell), it is usually found to present fewer conceptual difficulties than the integral invariant I.

INTRODUCTION

Considerable difficulties were encountered in the early attempts to map the measured intensities of trapped particles. The difficulties were chiefly due to the high spatial gradients in the intensities. At low altitudes in the inner zone for example, a change in the distance from the center of the earth of 3 percent results in an intensity change of over a factor of 10. The shape of the earth's field deviates more than 3 percent from any possible dipole representation, therefore attempts to use a dipole model for a coordinate system can be expected to produce rather chaotic results.

The present paper describes a coordinate system which not only takes account of the nondipole character of the field but can also be used to organize measurements along lines of force as is necessary for most theoretical studies.

ADIABATIC INVARIANTS

The use of adiabatic invariants in describing the motion of a particle in a magnetic field has been discussed by Northrup and Teller [1959]. In the present paper, the integral (or longitudinal) invariant at a point in space A is defined as $I = \oint_A^{A'} (1 - B_\ell/B)^{1/2} ds$ where ds is the differential path length along the line of force connecting the point A with its conjugate point A', B_ℓ is the magnitude of the magnetic field along the line of force, B is the magnitude of the magnetic field at the point A, and where the integral is to be taken along the line of force between the conjugate points. Defined in this manner, I can be considered to be a scalar field which has a definite value at each point in space and does not require reference to the motion of trapped particles. If there is no electric field, this definition is equivalent to $I = P^{-1} \oint_A^{A'} P_{\|} \, ds$ where P is the total momentum of a particle which mirrors at the point in space A and where $P_{\|}$ is the component of momentum along the line of force. If we assume that all three adiabatic invariants are

conserved for a given particle, then the values of I are the same at every point in space at which a given particle mirrors. If the energy and mirror point distributions of a set of trapped particles in time equilibrium do not change importantly during the time the slowest particles drift once around the earth (for example, the high energy protons in the inner zone), then the directional intensity perpendicular to the line of force will be the same at all points in space which have the same values of B and I.

MAGNETIC SHELLS

The points in space which have the same value of B and I form a ring in each hemisphere. A particle mirroring at this B and I will remain upon the surface (or "shell") described by the lines of force which connect these rings.

Now in general, two particles which initially mirror at different values of B along a particular line of force will not drift in longitude to the same lines of force. This means that the shells described by the trajectories of the two particles do not coincide. It will be shown however, that in the earth's magnetic field, this effect is relatively small. One important consequence of this fact is that the omnidirectional intensity as well as the directional intensity is constant along the loci of constant B and I.

DEFINITION OF THE MAGNETIC SHELL PARAMETER L

The fact that all particles which drift through a given line of force will remain on approximately the same shell throughout their motion leads immediately to the desirability of finding a method of labelling all points in space with a number which is unique for each shell.

Each locus of constant B and I is a line which lies on a fixed shell. Any parameter which is a function of only B and I will therefore have the correct longitude dependence. The problem of defining a magnetic shell parameter is thus reduced to finding a function f(B,I) which is constant along lines of force. Such a function could be found empirically by examining the functions $I_i = g_i(B)$ along lines of force calculated with a representation of the earth's field. An empirical fit is not necessary however, because the average of the functions $g_i(B)$ around a shell is well represented by the function obtained for a dipole field.

The integral invariant in a dipole field at a magnetic latitude λ on a line of force which has an equatorial radial distance of R_o is given by

$$I = 2R_o \int_0^Y \left\{ 1 - \left[\left(\frac{1+3Y_a^2}{1+3Y^2} \right) \left(\frac{1-Y^2}{1-Y_a^2} \right)^3 \right]^{1/2} \right\} (1+3Y_a^2)^{1/2} dY_a \tag{1}$$

or

$$I = R_o h_1(\lambda) \tag{2}$$

where $Y = \sin \lambda$. Now in a dipole field

$$B = \frac{M}{R_o^3 \cos^6 \lambda} (1 + 3 \sin^2 \lambda)^{1/2} \tag{3}$$

where M is the dipole magnetic moment. By (3) we see that

$$R_o^3 B/M = h_2(\lambda) \tag{4}$$

Equations (2) and (4) give

$$I^3 B/M = R_o^3 B/M \; h_1^3(\lambda) = R_o^3 B/M \; h_3(R_o^3 B/M)$$

$$= h_4(R_o^3 B/M)$$

or

$$R_o^3 B/M = F(I^3 B/M) \tag{5}$$

The magnetic shell parameter L is now defined for a point in the earth's magnetic field by the

equation

$$L^3B/M = F(I^3B/M) \tag{6}$$

where I and B are to be calculated for the point with a representation of the earth's field, M is the dipole moment of the earth* and F is the function in equation (5) which is calculated with a dipole field.

A set of values for the function F is given in Table I. For accurate computation of L, the following method can be used:

Let

$$\ln\left(\frac{L^3B}{M} - 1\right) = \sum_{n=0}^{n=6} a_n X^n \tag{7}$$

where $X = \ln(I^3B/M)$. Sets of the coefficients a_n for different ranges of X are given in Table II. This method introduces an error in L of less than 0.3 percent for $-\infty < X < \infty$ and less than 0.03 percent for $X < 10$.

* The value $M = 8.06 \times 10^{25}$ gauss $cm^3 = 0.311653$ gauss R_e^3 (R_e = 6371.2 km) has been found to be satisfactory.

SIGNIFICANCE OF L

In general, L should be regarded as a parameter which retains most of the useful properties of I exactly and which is also approximately constant along lines of force. To gain some feeling for the meaning of L, it is useful to remember that in the case of a pure dipole field, a magnetic shell is labelled by an L equal to the shell's equatorial radius.

For most purposes, B and L should be used as the principal spatial coordinates. For studies involving intuition, it is sometimes desirable to use a coordinate system which has a closer resemblance to the actual physical geometry. One system of this kind can be obtained by transforming B and L to polar coordinates using the dipole relations

$$B = \frac{M}{R^3}\left(4 - \frac{3R}{L}\right)^{1/2}, \quad R = L\cos^2\lambda. \tag{8}$$

This relationship is illustrated in Figure 1.

A great deal of caution must be exercised when using the coordinates R and λ obtained in this manner, because while the irregular characteristics of the magnetic field will in effect be removed, geographic coordinates will transform in an irregular longitude dependent manner.

VARIATION OF L ALONG LINES OF FORCE

Tables of I versus B along 1400 different lines of force were kindly supplied to the author by Messrs. D. C. Jensen, R. W. Murray, and J. A. Welch, Jr. These tables were computed with the 512 term spherical harmonic expansion (n = 24, m = 17) of the earth's field obtained by D. C. Jensen and W. A. Whitaker, [1960] and from the 1955 surface data. The L values obtained from these sets of B and I were found to vary less than one percent along most of the lines of force. Figure 2 shows the variation in L along six lines of force and includes several of the worst cases. The variations along different lines of force were found to be systematic in both latitude and longitude. This is illustrated in Figure 3 where the deviations in L, along lines forming the magnetic shells labelled by L = 1.2, 1.5, 2.2 and 3.0 earth radii, are plotted versus the geographic longitude at the northern ends of the lines. A positive deviation means that L increased toward higher values of B.

This kind of check upon the variation of L along lines of force tends to be independent of the

precision of the magnetic field analysis. An analysis of the earth's field based upon improved knowledge of the surface field would probably have nondipole terms of similar magnitude and therefore would be expected to give similar variations in L along lines of force. It should be noted however that in the present analysis, the contributions of external current systems have been assumed to be zero.

THE ARGUS SHELLS

Well defined shells of electrons injected by the three high altitude nuclear detonations Argus I, II and III were detected by Satellite 1958ε (Explorer IV) [Van Allen, et al., 1959]. Each of the observed intersections of the satellite trajectory with an Argus shell should have the same value of L. Figure 4 shows the L values obtained for the observed intersections as a function of geographic longitude. The average L values for the shells are 1.715, 2.115 and 2.16 earth radii for Argus I, II and III respectively. In addition to the scatter due to measurement inaccuracies, systematic variations with longitude of approximately ± 1.5 percent can be discerned. By comparison, Pennington [1961] has found that the trace of the data points in the northern hemisphere for Argus III projected upon the surface of the earth deviates more than ± 3.5 degrees from the earth trace of the best possible offset dipole shell. A latitude error of ± 3.5 degrees for the Argus III shell corresponds to an error in L of about ± 13 percent.

The range of B for the data points on each

shell is not large. The deviations of the L values in Figure 4 are therefore almost entirely due to inaccuracies in the surface field upon which the magnetic field representation is based. It is interesting to note that the deviations in the L values are largest in the regions where the discrepancies between the various available maps of the surface field are also large. No definite time dependence can be discerned in the data shown in Figure 4. An upper limit on the rate of change in L is 0.001 earth radii per day.

PROTON INTENSITIES IN THE INNER ZONE

The most complete set of data pertaining to the spatial distribution of particles in the inner zone presently available was obtained by the detectors on Satellite 1958 Epsilon [Van Allen, McIlwain and Ludwig, 1958]. The results of a preliminary analysis of the Geiger tube data are shown in Figures 5 and 6. The geometric factors and proton thresholds are approximately 0.54 cm^2 and 31 Mev for the unshielded counter and 0.62 cm^2 and 43 Mev for the shielded counter. Comparison with the scintillation counter data indicates that most of the Geiger tube counting rates were probably due to penetrating protons rather than bremsstrahlung from the very much higher fluxes of non-penetrating electrons.

The data points shown in Figures 5 and 6 were obtained from recordings made at stations in North and South America, Europe, Africa, Asia, Australia, New Zealand and Hawaii. Data obtained during the periods immediately following high altitude nuclear detonations have been excluded.

The general physical configuration of the lower part of the inner zone is illustrated in

Figures 7 and 8 where the B versus L curves in Figures 5 and 6 have been transformed into polar coordinates in the manner previously described. The dashed lines approximately represent the maximum excursions of the earth's surface in these coordinates.

Some of the aspects of these graphs which will be subjects for future papers include:

(a) Determination of angular distributions in the manner outlined by E. C. Ray [1960].

(b) The spatial dependence of proton injection and loss mechanisms.

(c) The spatial dependence of the proton energy spectrum.

(d) The time dependence of the intensities.

(e) Comparison with data obtained by instruments on other space vehicles.

SOLAR COSMIC RAYS

The application of the B and L coordinate system is by no means limited to trapped particles. In general, it can be usefully employed in the study of any phenomenon in which motion tends to be along lines of force. Some obvious examples are auroral particles, whistler mode wave propagation, and low energy cosmic rays.

The latitude dependence of solar cosmic rays is of particular interest in that it can be used to obtain information about both the energy spectrum of the particles and the distortion of the earth's magnetic field by external current systems. An example of the latitude dependence of solar cosmic rays is shown in Figure 9. The left side of this figure shows the intensity versus time measured by the shielded Geiger counter aboard Satellite 1959 Iota (Explorer VII) during a solar cosmic ray event and the right side shows the same data points plotted versus L.

TIME VARYING MAGNETIC FIELD

The magnetic shells labelled by L values greater than 3 earth radii are probably distorted by an important amount during magnetic storms. It would be difficult if not impossible to calculate true instantaneous values of I during a magnetic storm. It is suggested that the values calculated for magnetically quiet periods be used as a fixed reference system in which the perturbations on the various phenomena can be studied.

COMPUTATION OF I

Direct evaluation of $I = \oint (1 - B_\ell/B)^{1/2} ds$ entails a considerable amount of computation. A number of relatively fast methods of computing I have been devised. At least one of these methods (which in general involve various means of interpolation) will probably be made available in the form of a computer program written in the Fortran language.

CONCLUSION

The choice of B and L as the primary coordinates is of course quite arbitrary. One possible alternate for B is $B/B_o = L^3B/M$ where $B_o = M/L^3$ is the equatorial value of B on the line of force. It should be noted that any pair of the quantities B, L, R, λ and B/B_o can be used in place of B and L. To avoid confusion and to facilitate the comparison of different sets of data, it is suggested that a pair of coordinates other than B and L be employed only if a substantially improved presentation is obtained.

ACKNOWLEDGEMENTS

I would like to thank Professor J. A. Van Allen and Professor E. C. Ray for their suggestions and helpful discussions. I would also like to thank Captain J. A. Welch, Jr., Mr. D. C. Jensen and others at the Air Force Special Weapons Center for furnishing many of the necessary computations.

This research is supported in part by the Office of Naval Research (contract number N9onr 93803) and by the National Aeronautics and Space Administration (contract number NASw-17).

REFERENCES

Jensen, D. C. and W. A. Whitaker, "A Spherical Harmonic Analysis of the Geomagnetic Field", J. Geophys. Research 65, 2500 (1960).

Northrup, J. G. and E. Teller, "Stability of the Adiabatic Motion of Charged Particles in the Earth's Magnetic Field", Phys. Rev. 117, 215-225 (1960).

Pennington, R. H., "Equation of a Charged Particle Shell in a Perturbed Dipole Field", J. Geophys. Research 66, 709-712 (1961).

Ray, E. C., "On the Theory of Protons Trapped in the Earth's Magnetic Field", J. Geophys. Research 65, 1125-1134 (1960).

Van Allen, J. A., C. E. McIlwain and G. H. Ludwig, "Radiation Observations with Satellite 1958ϵ", J. Geophys. Research 64, 271-286 (1959-a).

Van Allen, J. A., C. E. McIlwain and G. H. Ludwig, "Satellite Observations of Electrons Artificially Injected into the Geomagnetic Field", J. Geophys. Research 64, 877-891 (1959-b).

FIGURE CAPTIONS

Figure 1. The mapping of the polar coordinates R and λ on to the B,L plane according to the transformation

$$B = \frac{M}{R^3}\left(4 - \frac{3R}{L}\right)^{1/2}, \quad R = L\cos^2\lambda.$$

Figure 2. The variation in L along six lines of force. Several of the worst cases are included.

Figure 3. The maximum deviation in L along lines forming magnetic shells labelled by L = 1.2, 1.5, 2.2 and 3.0 earth radii plotted versus the geographic longitude at the northern ends of the lines. A positive deviation means that L increased toward higher values of B.

Figure 4. The L values for the observed intersections of the Explorer IV trajectory with the three Argus shells are plotted versus geographic longitude.

Figure 5. Contours of constant true counting rate of the unshielded Geiger counter in Explorer IV. The points shown correspond to data obtained over a wide range of geographic latitude and longitude.

Figure 6. Contours of constant true counting rate of the shielded Geiger counter in Explorer IV.

Figure 7. The contours of constant counting rate shown in Figure 5 transformed to the polar coordinates R and λ.

FIGURE CAPTIONS
(continued)

Figure 8. The contours of constant counting rate shown in Figure 6 transformed to the polar coordinates R and λ.

Figure 9. The left side of this figure shows the omnidirectional intensity measured by the shielded Geiger counter aboard Explorer VII as a function of time during a solar cosmic ray event. The right side of the figure shows the same data points plotted versus L. On some occasions the modification of the earth's field by external current systems permits solar particles to arrive along lines of force labelled by considerably lower L values.

TABLE I

I^3 B/M	L^3 B/M	I^3 B/M	L^3 B/M
2.37529×10^{-15}	1.00002	1.93121×10^{-3}	1.17553
1.72697×10^{-12}	1.00016	2.65795×10^{-3}	1.19618
3.70298×10^{-11}	1.00045	3.60595×10^{-3}	1.21827
2.37086×10^{-9}	1.00180	4.82943×10^{-3}	1.24187
2.70390×10^{-8}	1.00406	6.39281×10^{-3}	1.26706
1.52215×10^{-7}	1.00722	8.37277×10^{-3}	1.29392
5.82114×10^{-7}	1.01131	1.08602×10^{-2}	1.32252
1.74352×10^{-6}	1.01632	1.39624×10^{-2}	1.35298
4.41257×10^{-6}	1.02228	1.78056×10^{-2}	1.38538
9.87364×10^{-6}	1.02919	2.25380×10^{-2}	1.41985
2.01130×10^{-5}	1.03707	2.83332×10^{-2}	1.45650
3.80506×10^{-5}	1.04596	3.53938×10^{-2}	1.49547
6.78113×10^{-5}	1.05585	4.39567×10^{-2}	1.53691
1.15049×10^{-4}	1.06680	5.42973×10^{-2}	1.58097
1.87314×10^{-4}	1.07881	6.67358×10^{-2}	1.62782
2.94482×10^{-4}	1.09194	8.16455×10^{-2}	1.67767
4.49250×10^{-4}	1.10620	9.94598×10^{-2}	1.73070
6.67702×10^{-4}	1.12165	1.20681×10^{-1}	1.78716
9.69961×10^{-4}	1.13832	1.45893×10^{-1}	1.84729
1.38095×10^{-3}	1.15626	1.75772×10^{-1}	1.91135

TABLE I
(continued)

I^3 B/M	L^3 B/M	I^3 B/M	L^3 B/M
2.11103×10^{-1}	1.97966	4.84816	4.85057
2.52798×10^{-1}	2.05255	5.67587	5.16095
3.01912×10^{-1}	2.13036	6.64657	5.50164
3.59672×10^{-1}	2.21352	7.78642	5.87648
4.27504×10^{-1}	2.30245	9.12680	6.28994
5.07058×10^{-1}	2.39766	1.07055×10	6.74720
6.00263×10^{-1}	2.49967	1.25680×10	7.25432
7.09352×10^{-1}	2.60911	1.47699×10	7.81840
8.36934×10^{-1}	2.72664	1.73787×10	8.44781
9.86054×10^{-1}	2.85300	2.04766×10	9.15245
1.16025	2.98905	2.41655×10	9.94413
1.36367	3.13571	2.85705×10	1.08369×10
1.60116	3.29403	3.38471×10	1.18478×10
1.87843	3.46520	4.01899×10	1.29973×10
2.20216	3.65056	4.78427×10	1.43104×10
2.58020	3.85161	5.71146×10	1.58179×10
3.02183	4.07005	6.83985×10	1.75576×10
3.53799	4.30783	8.21991×10	1.95767×10
4.14164	4.56716	9.91695×10	2.19347×10

TABLE I
(continued)

I^3 B/M	L^3 B/M	I^3 B/M	L^3 B/M
1.20162×10^2	2.47069×10	1.62942×10^3	1.58767×10^2
1.46301×10^2	2.79896×10	1.90201×10^3	1.79669×10^2
1.79085×10^2	3.19079×10	2.23574×10^3	2.04483×10^2
2.20532×10^2	3.66255×10	2.64005×10^3	2.34175×10^2
2.45179×10^2	3.93495×10	3.14300×10^3	2.70014×10^2
2.73402×10^2	4.23601×10	3.76361×10^3	3.13689×10^2
3.05069×10^2	4.56967×10	4.55081×10^3	3.67477×10^2
3.41513×10^2	4.94049×10	5.54426×10^3	4.34504×10^2
3.82642×10^2	5.35387×10	6.83524×10^3	5.19133×10^2
4.30241×10^2	5.81615×10	8.51087×10^3	6.27578×10^2
4.84311×10^2	6.33486×10	1.07567×10^4	7.68892×10^2
5.47285×10^2	6.91896×10	1.37789×10^4	9.56603×10^2
6.19343×10^2	7.57921×10	1.79974×10^4	1.21153×10^3
7.03884×10^2	8.32855×10	2.39555×10^4	1.56683×10^3
8.01427×10^2	9.18267×10	3.27489×10^4	2.07743×10^3
9.16824×10^2	1.01607×10^2	4.60402×10^4	2.83877×10^3
1.05125×10^3	1.12862×10^2	6.73169×10^4	4.02645×10^3
1.21182×10^3	1.25883×10^2	1.02942×10^5	5.98740×10^3
1.40095×10^3	1.41032×10^2	1.67841×10^5	9.47159×10^3

TABLE I
(continued)

I^3 B/M	L^3 B/M	I^3 B/M	L^3 B/M
2.96984×10^5	1.63048×10^4	4.09266×10^7	2.00752×10^6
5.95512×10^5	3.17247×10^4	1.91226×10^8	9.28013×10^6
1.44453×10^6	7.49153×10^4	6.50554×10^8	3.12969×10^7
5.00559×10^6	2.51887×10^5	5.20779×10^9	2.50188×10^8
1.47748×10^7	7.32706×10^5		

TABLE II

	$X < -16$	$-16 < X < 0$	$0 < X < 8$	$8 < X < 21$	$X > 21$
a_0	0.294	0.62290	0.62291	1.0824	-3.04
a_1	0.330	0.43351	0.43416	0.20395	1.00
a_2	0	1.4495×10^{-2}	1.3680×10^{-2}	5.4145×10^{-2}	0
a_3	0	1.2154×10^{-3}	1.4784×10^{-3}	-9.3218×10^{-4}	0
a_4	0	5.9474×10^{-5}	1.2413×10^{-5}	-5.6831×10^{-5}	0
a_5	0	1.5367×10^{-6}	-8.1278×10^{-6}	2.7879×10^{-6}	0
a_6	0	1.5843×10^{-8}	1.4604×10^{-7}	-3.4751×10^{-8}	0

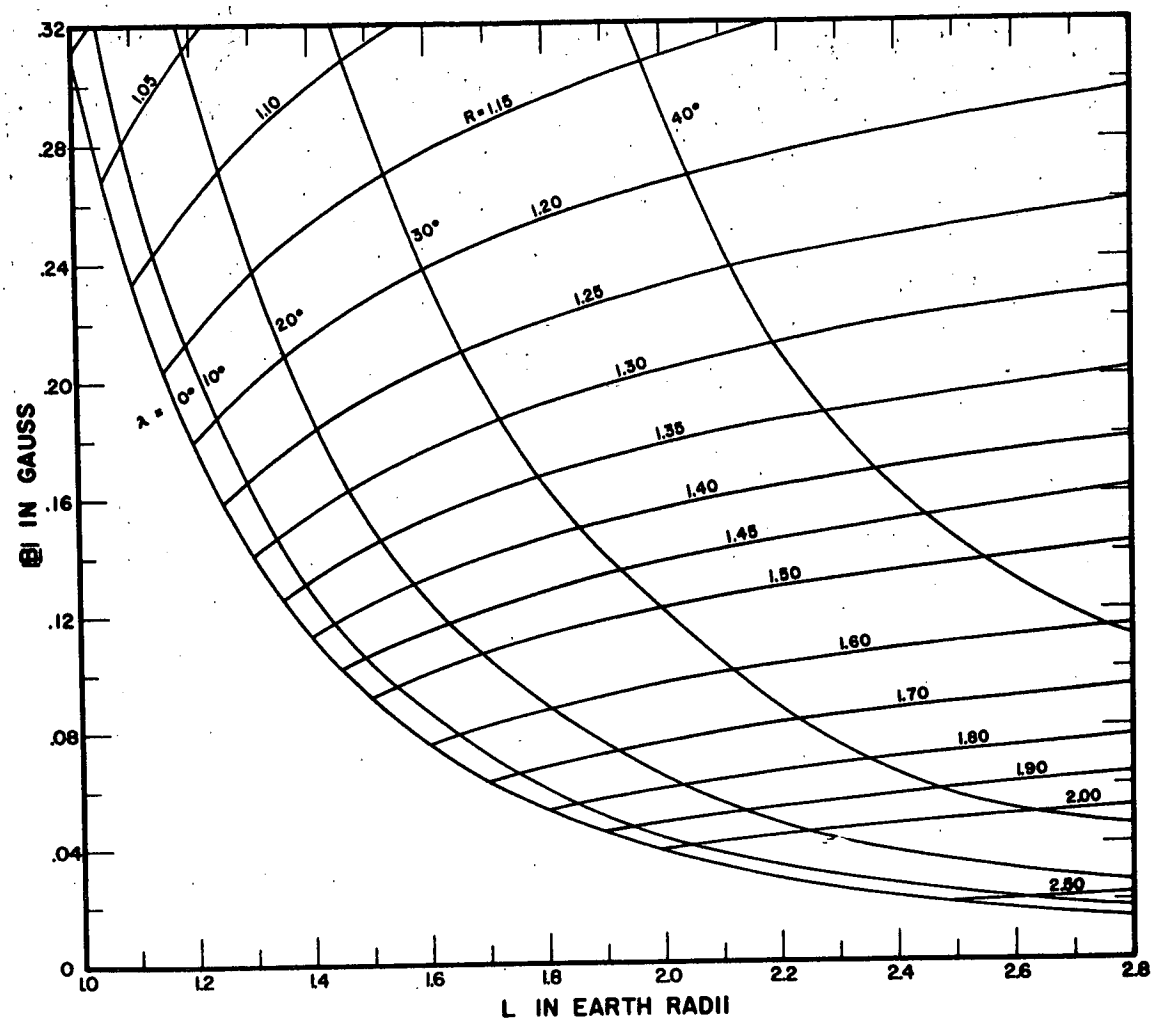
.32
.28
.24
.20
.16
.12
.08
.04
0
|B| IN GAUSS
1.0
1.2
1.4
1.6
1.8
2.0
2.2
2.4
2.6
2.8
L IN EARTH RADII
λ = 0°
10°
20°
30°
40°
1.05
1.10
R=1.15
1.20
1.25
1.30
1.35
1.40
1.45
1.50
1.60
1.70
1.80
1.90
2.00
2.50

Figure 1

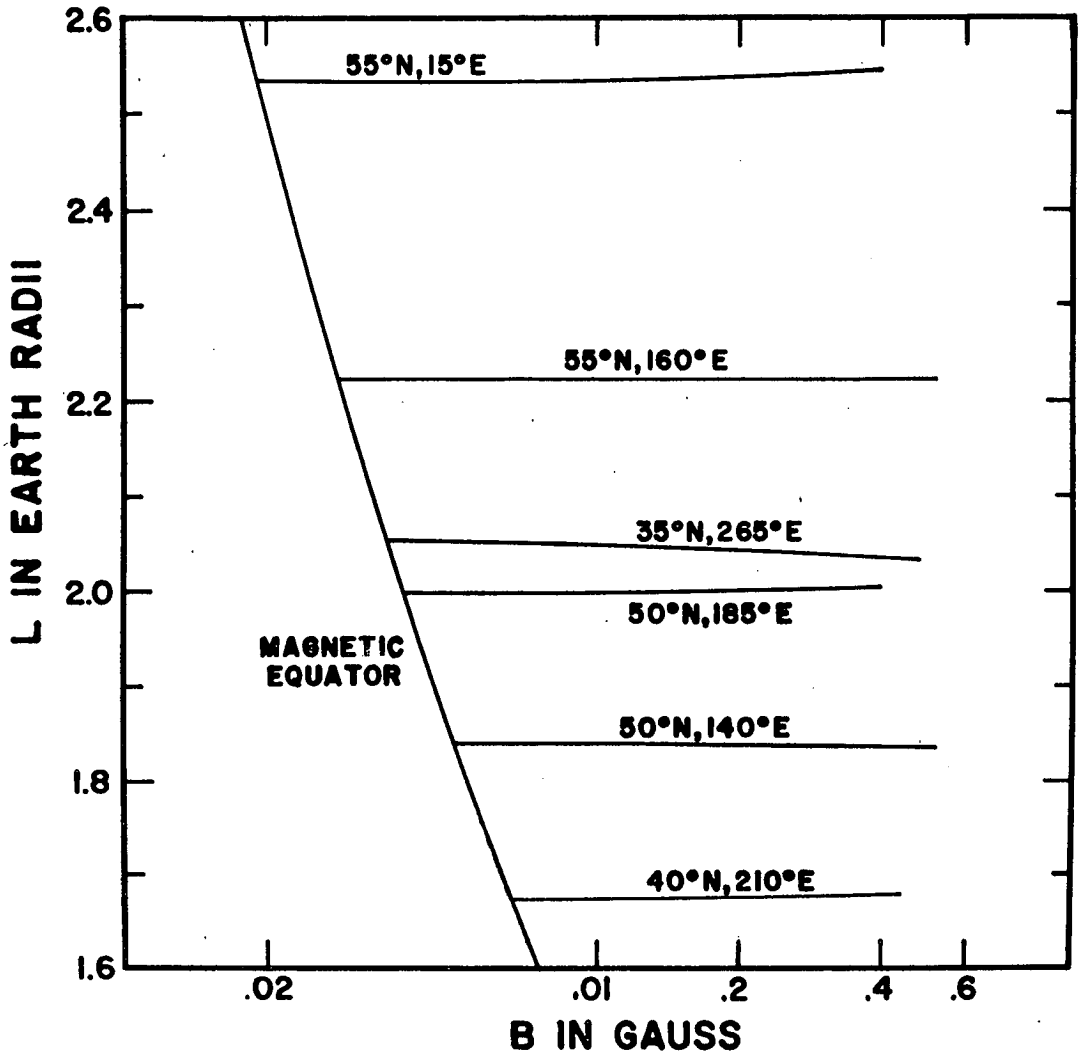
2.6
2.4
2.2
2.0
1.8
1.6
L IN EARTH RADII
55°N, 15°E
55°N, 160°E
35°N, 265°E
50°N, 185°E
MAGNETIC EQUATOR
50°N, 140°E
40°N, 210°E
.02
.01
.2
.4
.6
B IN GAUSS

Figure 2

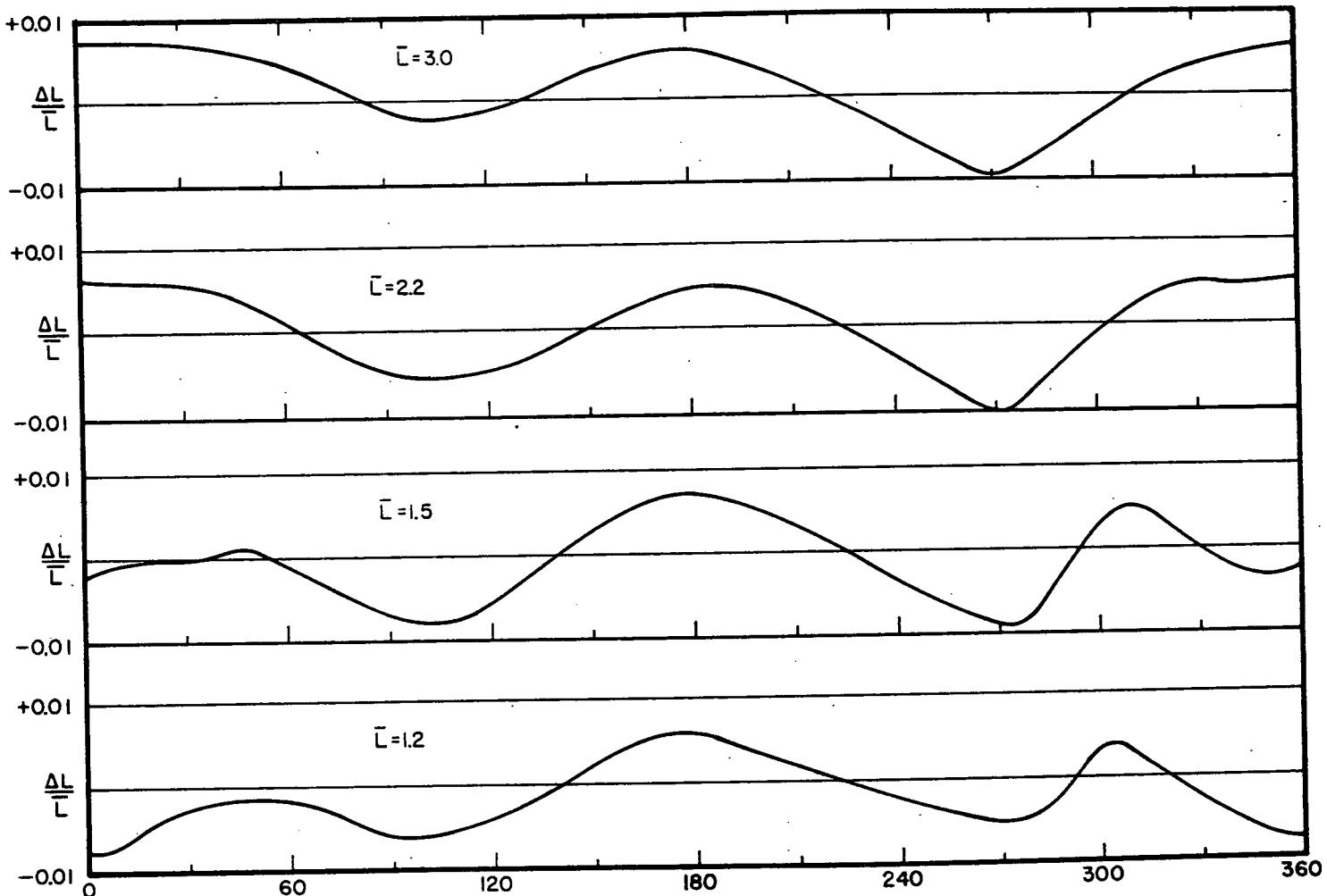
+0.01
ΔL/L
-0.01
L̄=3.0
+0.01
ΔL/L
-0.01
L̄=2.2
+0.01
ΔL/L
-0.01
L̄=1.5
+0.01
ΔL/L
-0.01
L̄=1.2
0
60
120
180
240
300
360
LONGITUDE AT NORTHERN END OF THE LINES OF FORCE

Figure 3

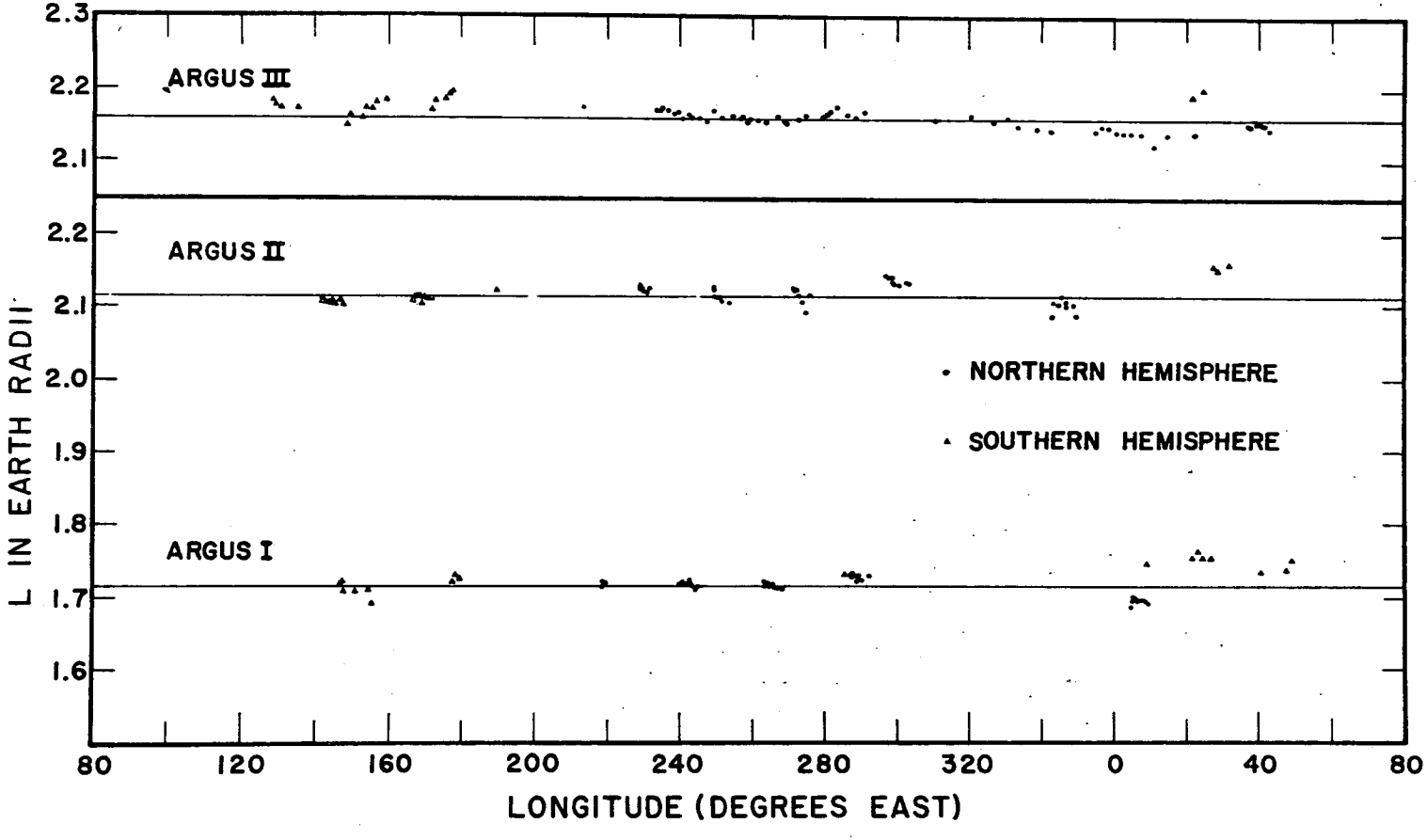
2.3
2.2
2.1
2.2
2.1
2.0
1.9
1.8
1.7
1.6
L IN EARTH RADII
ARGUS III
ARGUS II
ARGUS I
• NORTHERN HEMISPHERE
▲ SOUTHERN HEMISPHERE
80
120
160
200
240
280
320
0
40
80
LONGITUDE (DEGREES EAST)

Figure 4

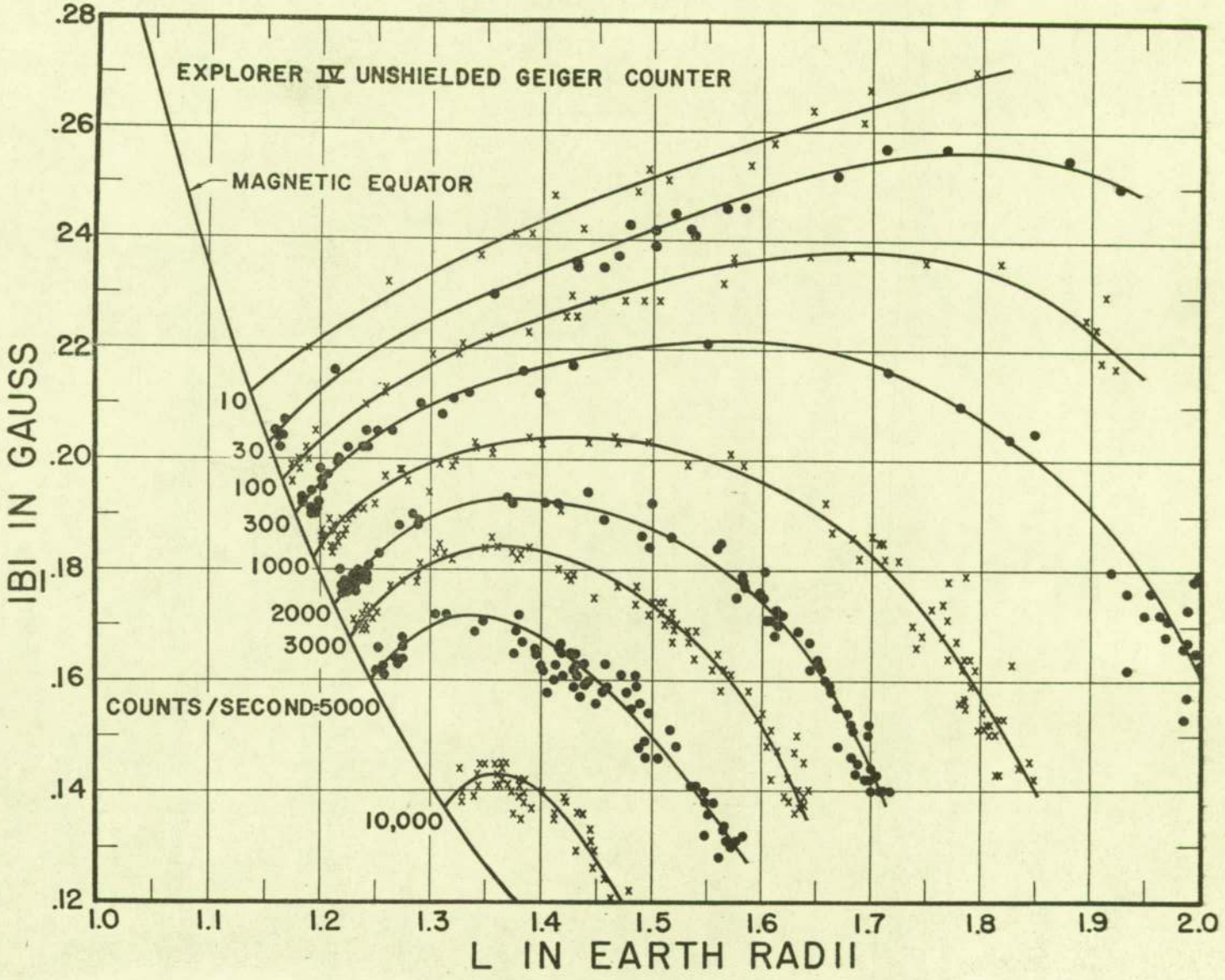
EXPLORER IV UNSHIELDED GEIGER COUNTER
MAGNETIC EQUATOR
10
30
100
300
1000
2000
3000
COUNTS/SECOND=5000
10,000
|B| IN GAUSS
.28
.26
24
22
.20
.18
.16
.14
.12
1.0
1.1
1.2
1.3
1.4
1.5
1.6
1.7
1.8
1.9
2.0
L IN EARTH RADII

Figure 5

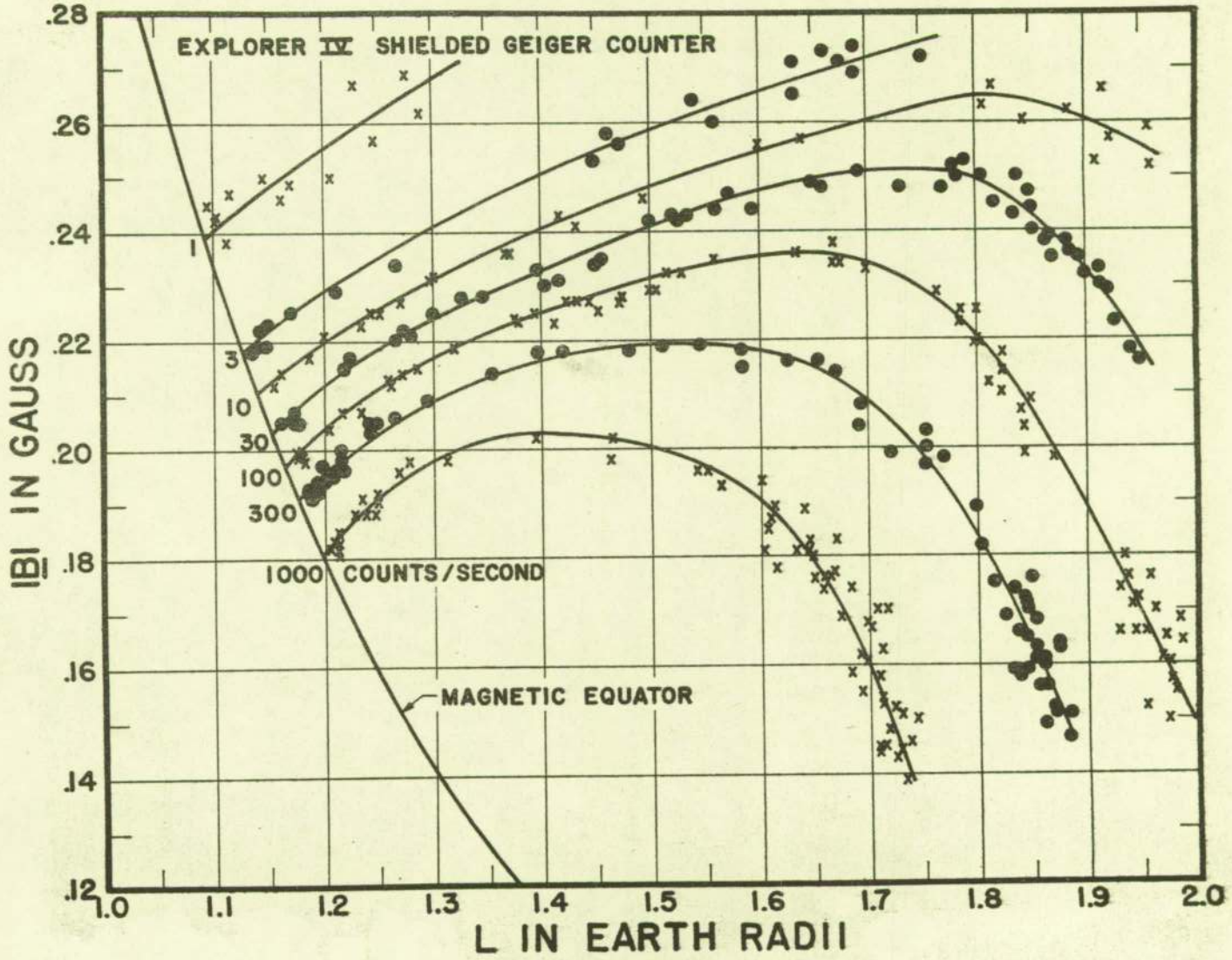
EXPLORER IV SHIELDED GEIGER COUNTER
1
3
10
30
100
300
1000 COUNTS/SECOND
MAGNETIC EQUATOR
|B| IN GAUSS
.28
.26
.24
.22
.20
.18
.16
.14
.12
1.0
1.1
1.2
1.3
1.4
1.5
1.6
1.7
1.8
1.9
2.0
L IN EARTH RADII

Figure 6

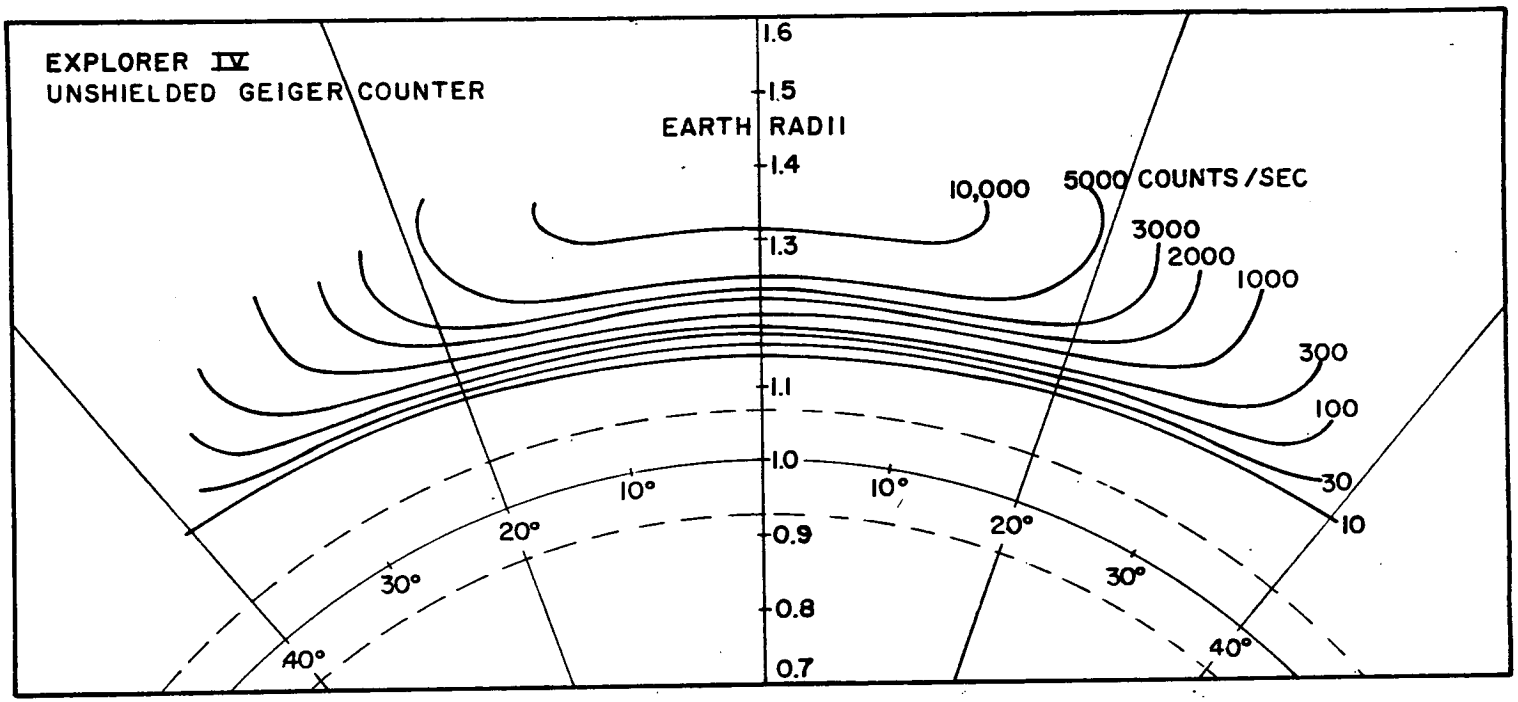
EXPLORER IV
UNSHIELDED GEIGER COUNTER
EARTH RADII
1.6
1.5
1.4
1.3
1.1
1.0
0.9
0.8
0.7
10,000
5000 COUNTS/SEC
3000
2000
1000
300
100
30
10
10°
10°
20°
20°
30°
30°
40°
40°

Figure 7

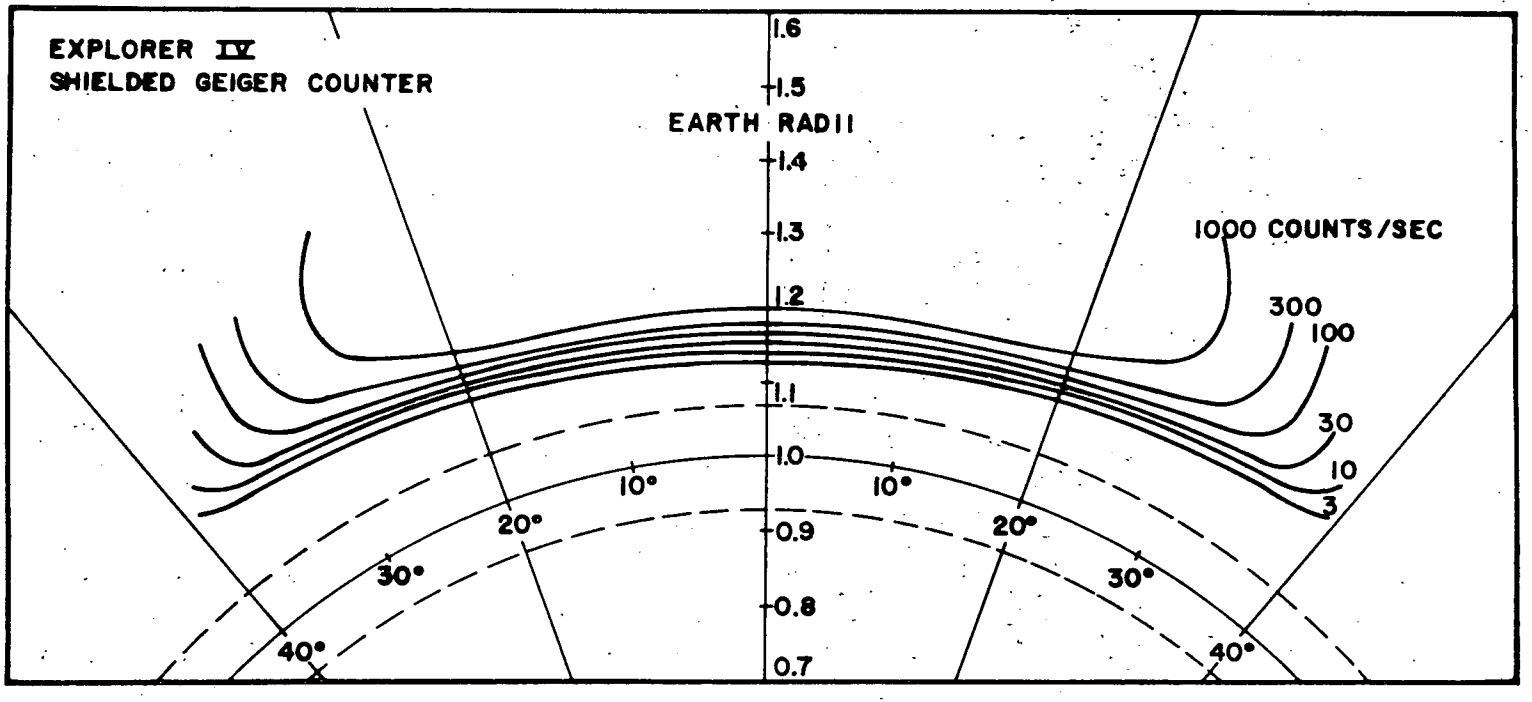
EXPLORER IV
SHIELDED GEIGER COUNTER
EARTH RADII
1.6
1.5
1.4
1.3
1.2
1.1
1.0
0.9
0.8
0.7
1000 COUNTS/SEC
300
100
30
10
3
10°
20°
30°
40°
10°
20°
30°
40°

Figure 8

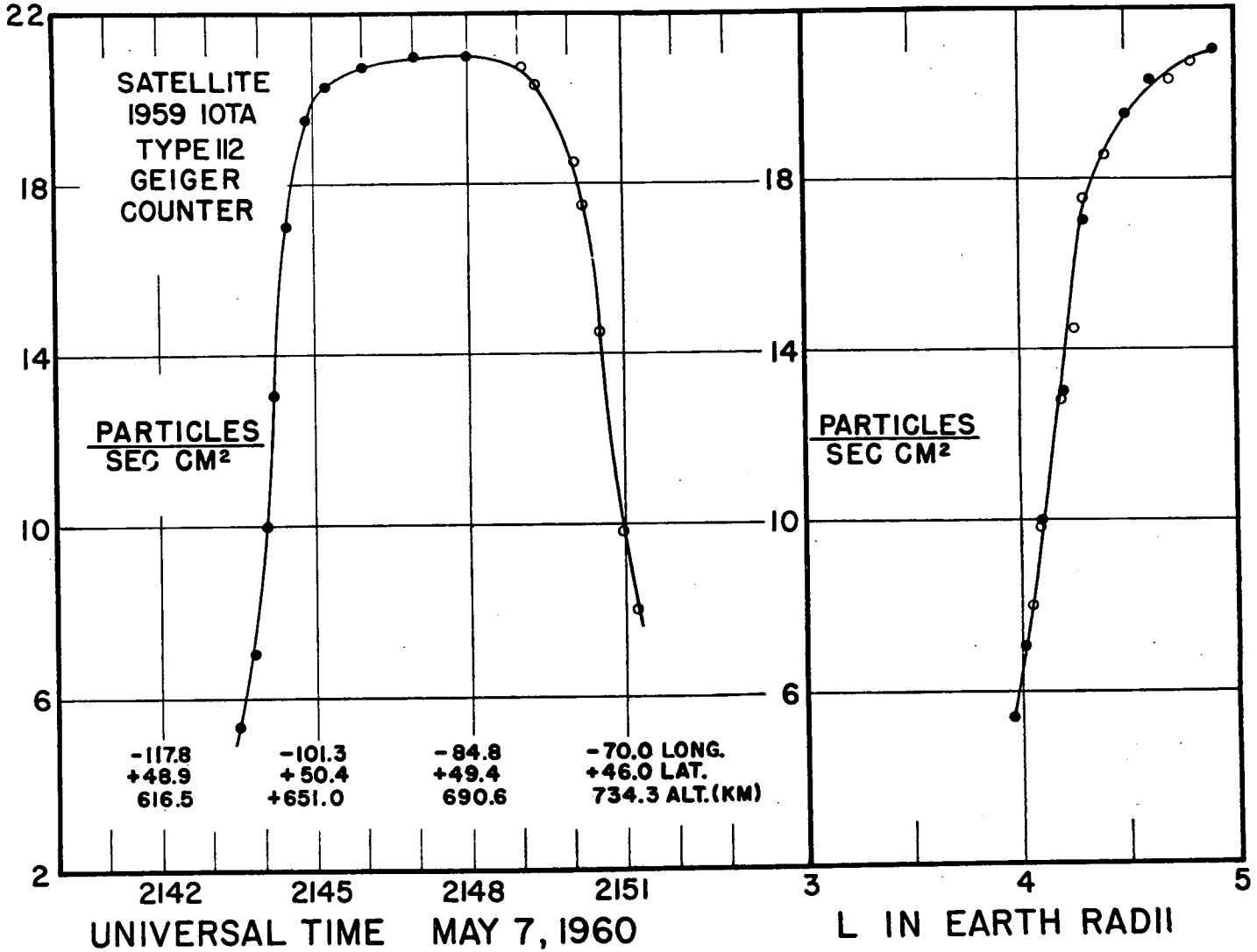
SATELLITE
1959 IOTA
TYPE 112
GEIGER
COUNTER
PARTICLES
SEC CM²
22
18
14
10
6
2
-117.8
+48.9
616.5
-101.3
+50.4
+651.0
-84.8
+49.4
690.6
-70.0 LONG.
+46.0 LAT.
734.3 ALT.(KM)
2142
2145
2148
2151
UNIVERSAL TIME MAY 7, 1960
PARTICLES
SEC CM²
3
4
5
L IN EARTH RADII

Figure 9